

Article

# Cerebral Organoids Derived from a Parkinson's Patient Exhibit Unique Pathogenesis from Chikungunya Virus Infection when Compared to a Non-Parkinson's Patient

Emily M Schultz<sup>1</sup>, TyAnthony J. Jones<sup>1</sup>, Sibe Xu<sup>1</sup>, Dana D. Dean<sup>1</sup>, Bernd Zechmann<sup>2</sup>, Kelli L. Barr<sup>1\*</sup>

1 Baylor University, Department of Biology, Waco, TX, USA

2 Center for Microscopy and Imaging, Baylor University, Waco, TX, USA

\* Correspondence: kelli\_barr@baylor.edu

**Abstract:** Arboviruses of medical and veterinary significance have been identified on all 7 continents with every human and animal population at risk for exposure. Like arboviruses, chronic neurodegenerative diseases like Alzheimer's and Parkinson's disease are found wherever there are humans. Viral parkinsonism has been documented for a variety of human pathogens though there are few studies that evaluate the effects of viral infection on degenerative neurological diseases. Significant differences in baseline gene and protein expression have been determined between Human Induced Pluripotent Stem Cell lines derived from a non-Parkinson's disease individual and from an individual with reported Parkinson's disease. While the organoids generated from each cell line were physically indistinguishable, significant differences were observed in gene and protein expression for neurotransmission and immunity. It was hypothesized that these inherent differences would impact cerebral organoid responses to viral infection. In this preliminary observational study, cerebral organoids from a non-Parkinson's and Parkinson's patient were infected with Chikungunya virus and observed for 2 weeks. Parkinson's organoids lost mass and exhibited a dysfunctional antiviral response. Neurotransmission data from both non-Parkinson's and Parkinson's organoids had dysregulation of IL-1, IL-10, IL-6. These cytokines are associated with mood and could be contributing to persistent depression seen in patients following CHIKV infection. Both organoid types had increased expression of CCR5 and CXCL10 which are linked to demyelination, highlighting a potential mechanism for virus-associated parkinsonism. The dysfunctional antiviral response of Parkinson's organoids highlights the need for more research in neurotropic infections in a neurologically compromised host.

**Keywords:** organoid, induced pluripotent stem cell, Parkinson's disease, neurotransmission, neuroimmunity, neuroinflammation, chikungunya, neuroinvasive.

---

## 1. Introduction

Arboviruses of medical and veterinary significance have been identified on all 7 continents with every human and animal population at risk for exposure. There are over 100 medically relevant arboviruses recognized and anyone who experiences an insect bite is at risk for exposure. Medically significant arboviruses are commonly found in the Togaviradea,

Bunyaviradea, and Flaviviradea families. These families contain viruses that cause encephalitis or hemorrhagic fever, and vaccines or treatments are not available for most infections. Death rates are roughly 20,000-50,000 per year for any given virus [1]. While mortality rates are proportionately low to number of cases, the risk of permanent disability is as high as 50% [1]. Rising temperatures and alterations in precipitation patterns have driven the emergence of these viruses into new regions [2-5]. Often, when these viruses emerge, new symptoms and increased pathology occur [6-11].

Infected individuals present with a spectrum of disease ranging from subclinical to death. The role of chronic diseases on intrinsic and innate immune defense is emerging as a significant player in a patient's ability to respond with viral infections [12-15]. Clinical studies have shown that viral infections can induce expression of pro-inflammatory cytokines that can impact mood and neurocognitive performance [16-18]. Taken together, these studies show that the genetic background of the host can impact the severity and duration of sequelae.

Like arboviruses, chronic neurodegenerative diseases like Alzheimer's and Parkinson's disease are found wherever there are humans. Viral parkinsonism has been documented for a variety of human pathogens though there are few studies that evaluate the effects of viral infection on degenerative neurological diseases [1]. Post-viral Parkinsonism has been documented for several viruses including Dengue virus [19], West Nile virus [20], Japanese Encephalitis virus [21], and St. Louis Encephalitis virus [22]. Symptoms of this condition include bradykinesia, tremor, ptosis, facial twitching, myoclonus, catatonia, and loss of speech [1,23]. Imaging studies often report a lack of Lewy bodies and the presence of neurofibrillary tangles usually associated with Alzheimer's disease [1].

How viruses cause parkinsonism is not known. Animal models of neurological infections do not translate to nor mimic changes in the human cerebral cortex documented in postmortem reports and imaging studies. Pathology reports have found complement proteins, MxA with Lewey bodies, and swollen neural processes [19,24]. MRI studies have reported changes in the *substantia nigra* [1]. Evaluation of central spinal fluid and rodent studies indicate that an inappropriate neuroimmune response is responsible [25]. These pathologies are also seen in patients with Parkinson's disease (PD) and multiple studies have shown that PD patients have dysregulation of multiple neuroimmune factors [25]. This begs the question of how a virus might affect an individual with or with a predisposition to PD.

While developing a cerebral organoid model derived from human induced pluripotent stem cells (hiPSC), it was discovered that significant differences in baseline genetic expression and protein expression exist between hiPSC lines derived from an individual with no reported illnesses and from an individual with reported PD. While the organoids were physically indistinguishable, significant differences were observed in gene and protein expression for neurotransmission and immunity [26]. We hypothesized that these differences would impact cerebral organoid response to viral infection. This study aimed to

classify those differences in response to infection with Chikungunya virus (CHIKV) so we might begin to understand how dysfunction in intrinsic and innate defenses could impact patient outcomes after infection with neurotropic arboviruses.

## 2. Materials and Methods

### 2.1 Cell Culture and Virus Propagation

Human induced pluripotent stem cells (ATCC ACS-1019) and human induced pluripotent stem cells with a genetic background of Parkinson's Diseases (ATCC ACS-1013) were both cultured in mTeSR1 media (StemCell Technologies) on plates coated with vitronectin XF (Stemcell Technologies) prior to organoid formation. *Cercopithecus aethiops* kidney cell line Vero E6 (ATCC CRL-1586) were grown in Dulbecco's modified Eagle's medium (DMEM) with 10% FBS, supplemented with penicillin/streptomycin, 1X non-essential amino acids, 1X Glutamax, and 1mM HEPES. All cell lines were incubated at 37°C/ 5% CO<sub>2</sub>. CHIKV (181/25) was obtained from BEI Resources (NR-50345) and expanded once in Vero cells. Infectious Units (IFU) and viral titers were measured via plaque assay.

### 2.2 Generation and Infection of Human Cerebral Organoids

Cerebral organoids were formed from hiPSC ACS-1019 and hiPSC ACS-1013 using the StemDiff Cerebral Organoid Kit (StemCell Technologies Cat #08570) and StemDiff Cerebral Organoid Maturation Kit (Cat. #08571 StemCell Technologies) following the manufacturer's directions. This methodology has been used for exploring pathologies for Alzheimer's disease [27] brain development [28] and a host of other applications [29]. Briefly, hiPSC were harvested with Gentle Cell Dissociation Reagent (StemCell Technologies Cat #07174) and then seeded into ultra-low attachment 96 well plates (Corning #7007) at a density of 9000 cells/well. Cells were seeded in seeding media containing Y-27632. On days 2 and 4, 100ul of Embryoid Body (EB) formation media was added to the wells. On day 5, EBs were observed to be rounded and tightly packed spheres about 200nm in size. EBs were embedded in Matrigel and incubated at 37°C for 1 hour. Embedded EBs were then placed in a 6 well, ultra-low attachment plate (StemCell Technologies Cat #3471) containing organoid expansion media. After three days, media was changed to maturation media. Media changes then occurred twice per week and cerebral organoids were matured for 53 days before data collection to allow for full maturation and to best resemble an adult brain [30,31].

At 53 days, organoids were transferred to ultra-low attachment 24 well plates at 1 organoid per well. Organoids were infected with 100,000 (~MOI 0.001) IFU per well. Controls included mock infected cerebral organoids. Supernatant was taken at 48h, 4 days, 7 days, 10 days, and 14 days post infection and pooled amongst similar treatments. Samples of cerebral organoid tissue were also taken, at 48h, 3 days, 7 days and 14 days post infection, and preserved in 4% paraformaldehyde solution in PBS (ThermoScientific CAT# J19943-K2) at 4°C.

### 2.3 Viral Quantification

Plaque assays were performed using the pooled supernatant samples from each treatment at each time point taken during the experiment following methods described elsewhere (Barr et al. 2018). Briefly, serial dilutions of virus in PBS were inoculated onto confluent Vero E6 cells and covered with 0.25% methylcellulose overlay. After 3 days, the overlay was removed, and cells were stained with Coomassie blue. For Quantitative Real-time PCR, RNA was extracted from all collected samples using a kit in accordance with the manufacturer's instructions (Zymo Quick Viral RNA kit). Virus was measured using Verso One-Step RT-qPCR Kit, SYBR Green, ROX (Thermo Fisher) and primers designed by Patel et al (2019) which are specific for the CHIKV E1 gene.

#### 2.4 Cerebral Organoid mRNA Extraction and Gene Expression

mRNA was extracted using Zymo Quick-RNA Kit (Zymo Research #R1052), and cDNA was generated using Applied Biosystems High-Capacity cDNA Reverse Transcription Kit (Applied Biosystems #4368814). Gene expression studies were then conducted using TaqMan Array Human Neurotransmitters (Applied Biosystems #4414094), TaqMan Array Human Immune Response (Applied Biosystems #4414204), and TaqMan Array Human Alzheimer's Disease (Applied Biosystems #4414070) with Applied Biosystems TaqMan Gene Expression Master Mix (Applied Biosystems #4369016). Results were analyzed using the  $\Delta\Delta\text{CT}$  method.

#### 2.5 Cerebral Organoid Size Measurements

Organoids were imaged using ImageQuant LAS 4000 with the bright field filter under high-resolution with automatic exposure. Organoid size was determined by using ImageJ (National Institutes of Health). The scale of the program was set to 13.9327 pixels/mm, and the area of each organoid was recorded. Results are expressed as an average between at least 12 organoids per treatment. ANOVA was performed to determine significance between PD and non-PD organoids. A Student's t-test was used to identify significance between organoids size pre-inoculation and at 13 days post infection.

#### 2.6 Immunofluorescence

Organoids were fixed in 4% paraformaldehyde in PBS (ThermoScientific Cat# J19943-K2) overnight at 4°C then cryoprotected in 30% sucrose prior to sectioning. After freezing samples at -80°C, organoid sections of 18 micrometers thick were produced using a cryomicrotome (CryoStar NX50, Thermo Fisher Scientific, Waltham, MA, USA). Afterwards organoid sections were blocked in 5% fetal sheep serum and primary staining was conducted overnight at 4°C (Table 1). Secondary staining was then conducted using fluorescent antibodies (Table 1) for 1 hour at 25°C. Slides were mounted with ProLong Gold Antifade Reagent with DAPI (Cell Signaling Technology #8961S). DAPI was used throughout to visualize nuclei and MAP2 was used to visualize microtubules to provide a structural reference. Chikungunya E2 monoclonal antibody CHK-48 (NR- 44002) was obtained from BEI resources and used to visualize CHIKV. Organoids were imaged using an Olympus Fluoview 3000 Confocal Laser Scanning Microscope (Olympus America Inc., Center Valley, PA, USA). All images were obtained using the same parameters including slices, laser power, gain, and offset.

Antibody	Host	Type	Source	Dilution
----------	------	------	--------	----------

Primary Antibodies				
Syntaxin 1A	Mouse	Monoclonal	Novus Biologicals	1:1000
Syntaxin 3	Rabbit	Polyclonal	Novus Biologicals	1:500
CYP46A1	Rabbit	Polyclonal	Invitrogen	1:500
ICAM-1/CD54	Mouse	Monoclonal	Novus Biologicals	1:1000
E-Selectin/CD62E	Mouse	Monoclonal	Novus Biologicals	1:1000
CCR7	Mouse	Monoclonal	Novus Biologicals	1:1000
NMDAR2C	Rabbit	Polyclonal	Novus Biologicals	1:1000
MAP2	Chicken	Polyclonal	Novus Biologicals	1:5000
NMDAR1	Mouse	Monoclonal	Novus Biological	1:1000
Synapsin 1	Rabbit	Polyclonal	Invitrogen	1:1000
SOX2	Mouse	Polyclonal	EMD Millipore	1:1000
Tuj1	Rabbit	Monoclonal	EMD Millipore	1:1000
Neurofilament	Mouse	Monoclonal	EMD Millipore	1:1000
Ubiquilin	Rabbit	Polyclonal	Novus Biologicals	1:1000
Capsase	Rabbit	Polyclonal	Novus Biologicals	1:1000
GFAP	Rabbit	Polyclonal	Novus Biologicals	1:1000
CHIKV CHK-48	Mouse	Monoclonal	BEI Resources	1:1000
Secondary Antibodies				
Anti-Chicken	Goat	Alexafluor 488	Novus Biologicals	1:3000
Anti-Rabbit	Goat	Alexafluor 594	Novus Biologicals	1:1000
Anti-Mouse	Goat	Alexafluor 647	Novus Biologicals	1:2000

**Table 1.** Antibodies used for immunofluorescence studies.

### 3. Results

#### 3.1 Size and morphology do not differ between organoids from non-PD and diseased backgrounds in response to CHIKV infection

There were no significant differences in organoid size post infection with CHIKV (Figure 1). Over the course of 12 days, PD organoids lost 0.6121 mm<sup>2</sup> ( $p = 0.0149$ ) while the size of non-PD organoids did not significantly differ between the day of inoculation (6.2454 mm<sup>2</sup>) to the 12<sup>th</sup> day post infection (p.i.) (6.5338 mm<sup>2</sup>) ( $p = 0.2855$ ). For all days of the experiment, PD and non-PD organoids did not differ in size ( $p = 0.0792-0.492$ )(Figure 1).

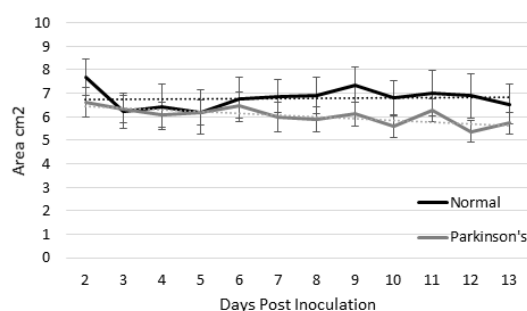
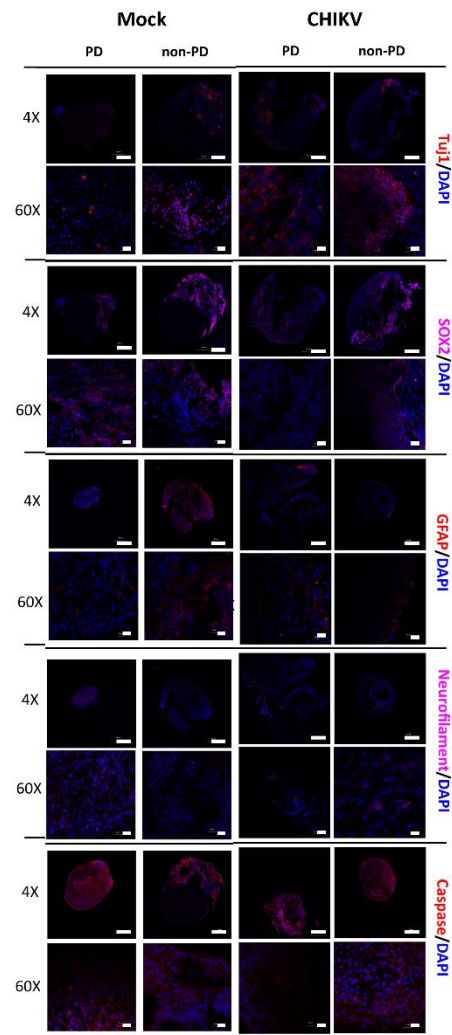
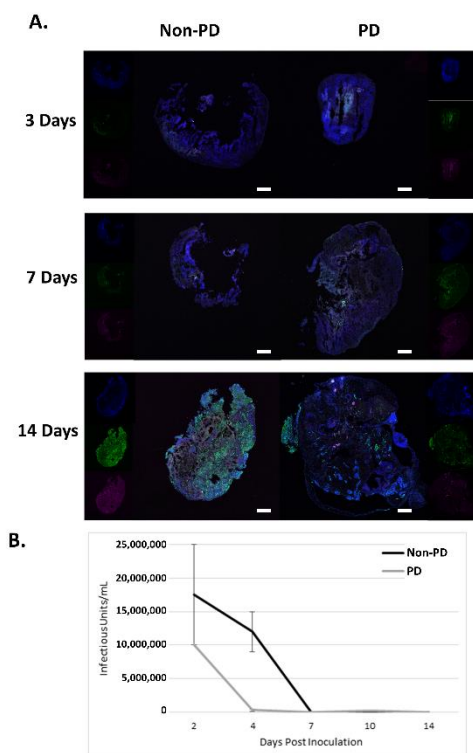


**Figure 1.** Impact of CHIKV on organoid size. Infected organoids were measured daily after inoculation. Non-PD organoids had no significant change in size over 12 days while PD organoids shrank an average of 0.6121 mm<sup>2</sup> ( $p = 0.0149$ ).



Immunofluorescence for morphology markers showed that both PD and non-PD organoids expressed SOX2, Tuj1, Neurofilament, and GFAP. SOX2 is expressed in proliferating neural progenitors and Tuj1 is a neuron-specific  $\beta$ -Tubulin. Both markers had increased fluorescence on the outer margins of the organoids indicating growth of new neurons in both infected and control organoids (Figure 2). GFAP or Glial fibrillary acidic protein is expressed by astrocytes and was found throughout non-PD organoids but PD organoids had less fluorescence (Figure 2). When CHIKV was present, more GFAP was seen in PD organoids while little GFAP was seen in non-PD organoids (Figure 2). Caspase was used to identify areas where development of brain tissue was present. Caspase was also used to visualize areas of cell death co-localized with virus. Caspase was seen in both PD and non-PD organoids with and without CHIKV (Figure 2).

**Figure 2.** Immunofluorescence for morphology markers. DAPI was used throughout to visualize nuclei and MAP2 was used to visualize microtubules to provide a structural reference. Images of organoids were obtained using an Olympus Fluoview3000 confocal microscope. Scale bar represents 500 nm for images obtained at 4X magnification and 20 nm for images obtained at 60X magnification.



Immunofluorescence was used to detect CHIKV over the course of 14 days. On days 3 and 7 p.i., CHIKV was detected evenly distributed in both organoid types. However, at 14 days p.i., CHIKV remained evenly distributed in non-PD organoids but had developed foci of infection in PD organoids (Figure 3A). Caspase was used as a marker for cell death which shows that viral distribution was co-localized with apoptosis in both organoid types (Figure 2). The viral titer and genome copies drastically decreased within the first 4 days of CHIKV infection for both organoid types (Figure

3B). The amount of viral genomic material decreased to undetectable levels by day 5 p.i. and was not detected on any timepoint following. Immunofluorescence however, detected CHIKV in both organoid types.

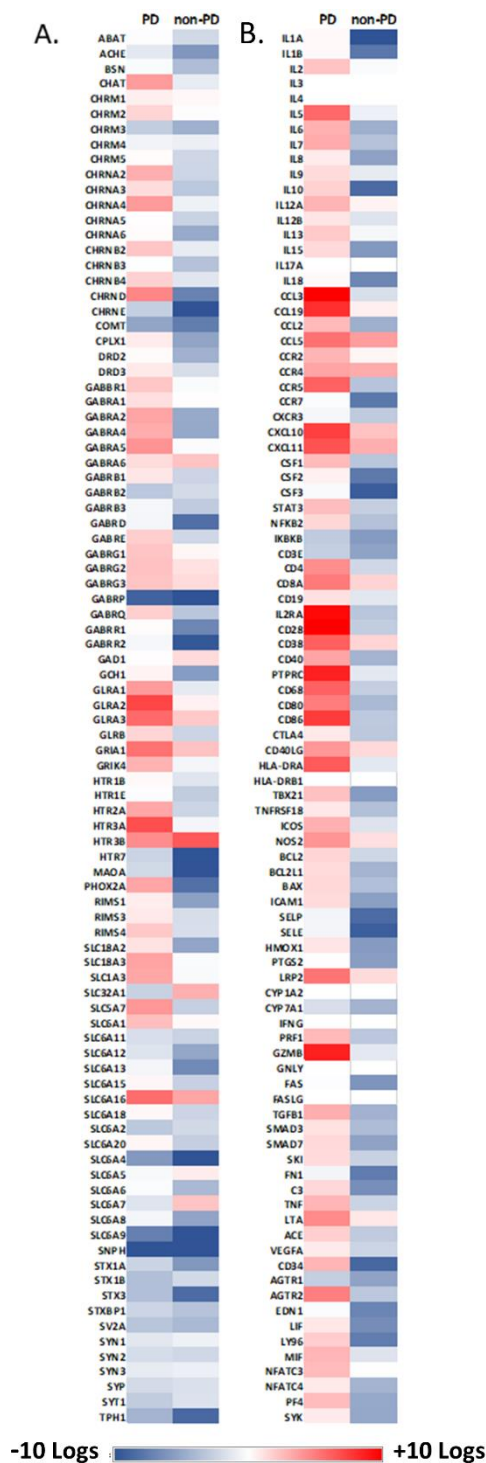


**Figure 3.** Chikungunya infection in PD and non-PD organoids. **A.** DAPI was used throughout to visualize nuclei, MAP2 was used to visualize microtubules to provide a structural reference and CHK-48 was used to visualize CHIKV. Images of organoids were obtained using an Olympus Fluoview3000 confocal microscope. Scale bar represents 500nm. **B.** CHIKV RNA decreased in both Non-PD and PD organoids, eventually becoming undetectable in PD organoids 4 days p.i., and after 7 days p.i. in Non-PD organoids.

*Non-PD and PD organoids exhibit unique responses to CHIKV infection*

$\Delta\Delta C_t$  comparison of Parkinson's and Non-PD organoids with a non-infected non-PD control showed unique expression patterns for each organoid type. Of 208 genes with significant changes in expression, both organoid types had similar patterns of expression (i.e. up or down-regulated) for 143 targets. 65 genes displayed opposite patterns of differential expression for both organoid types.

*3.2 Neurotransmission is reduced in Parkinson's organoids*

$\Delta\Delta C_t$  comparison of PD and non-PD organoids with their non-infected control showed that, global expression of neurotransmitters was down-regulated in PD organoids in response to CHIKV (Figure 4A, Table S1, S2). The data show that non-PD organoids exhibited increased expression of all targets associated with the cholinergic, serotonin, dopaminergic, GABA, glycine,

and glutamate neurotransmission (Figure 4A, Table S1, S2). Of note PHOX2A, SLC6A4, STX1, and STX3 were up-regulated in PD organoids but down-regulated in non-PD organoids. SLC6A7 had the greatest amount of down-regulation and STX3 had the greatest amount of up-regulation in PD organoids (Figure 4A, Table S1, S2). Non-PD organoids had the greatest up-regulation of HTR3B and the greatest down-regulation for GABARQ (Figure 4A, Table S1).

**Figure 4.** Differential expression of PD and non-PD organoids for genes associated with neurotransmission and immune response. RNA from 12 organoids per treatment was pooled and RT-PCR performed.  $\Delta\Delta\text{Ct}$  analysis was performed where CHIKV-infected PD and non-PD organoids were compared to their respective non-infected control organoids. **A.** Markers for neurotransmission **B.** Markers for immune response.

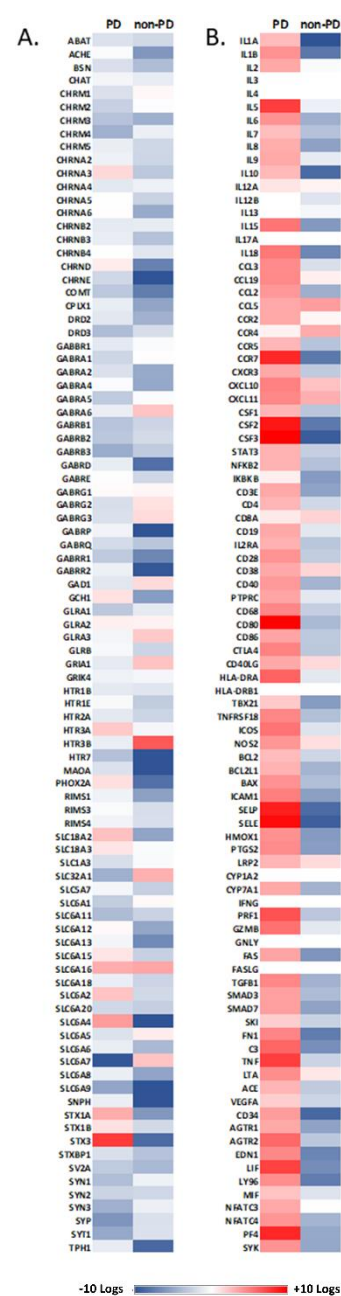
Since endogenous differences in expression exist for PD and non-PD cells [32-34], we performed  $\Delta\Delta\text{Ct}$  analysis pairing the infected PD organoids with the non-PD control. Thus, we were able to compare how PD and non-PD organoids differ from non-PD organoids in the presence of CHIKV. Here, expression of dopamine receptors DRD2 and DRD3 was down-regulated in non-PD organoids -4.5 and -1.9 logs, respectively but not differentially expressed in PD organoids in relation to the non-infected control (Figure 5A, Table S1, S3). Here, PDs organoids exhibited 3.5 log increased expression of dopamine receptor PHOX2A while non-PD organoids had decreased expression by -8.27 logs as determined by  $\Delta\Delta\text{Ct}$  comparison (Figure 5A, Table S1, S3).

Overall, markers associated with cholinergic neurotransmission displayed decreased expression in non-PD organoids while PD organoids tended to have no expression or increased expression of the same targets (Figure 5A, Table S1, S3). Of note CHRNA2 and CHRND were upregulated in PD organoids (3.15 and 4.72 logs, respectively) while non-PD organoids were down regulated -2.37 and -7.25 logs (Figure 5A, Table S1, S3).

Fourteen GABA receptors displayed significant differential expression for non-PD organoids and 13 receptors were differentially expressed in PD organoids (Figure 5A, Table S1, S3). 12 GABA receptors were down-regulated in non-PD organoids both in relation to PD organoids and the their non-infected control. GABRA2 was down-regulated -4.95 logs in non-PD organoids but upregulated 3.56 logs in PD organoids (Figure 5A, Table S1, S3). While GABRP was down-regulated in both organoid types, PD organoids were down-regulated -9.09 logs while non-PD organoids were down regulated -13.2 (Figure 5A, Table S1, S3).

Four glycine receptors (GLRA1, GLRA2, GLRA3, and GLRB) showed increased expression for both PD organoids when compared with the non-PD non-infected control. While reduced expression was observed in non-PD organoids both in relation to housekeeping gene and in relation to PD organoids (Figure 5A, Table S1, S3). Both organoid types had decreased expression of GLS with PD organoids down-regulated -1.8 logs and non-PD organoids down-regulated -7.2 logs (Figure 5A, Table S1, S3).

**Figure 5.** Differential expression of PD and non-PD organoids for neurotransmission and immune response associated genes. RNA from 12 organoids per treatment was pooled and RT-PCR performed.  $\Delta\Delta C_t$  analysis was performed where CHIKV-infected PD and non-PD organoids were compared to non-infected non-PD organoids. **A.** Markers for neurotransmission **B.** Markers for immune response.



Six glutamate receptors were evaluated, and PD organoids exhibited decreased expression of all targets over non-PD organoids when comparing their  $\Delta\Delta C_t$  values to their respective non-infected controls (Figure 4A, Table S1, S2, S3). Of note, GRIN1 and GRIN2B was up-regulated in PD organoids (4.32 and 5.42 logs) but down-regulated in non-PD organoids -4.28 and -4.02 logs, respectively (Figure 5A, Table S1, S3).

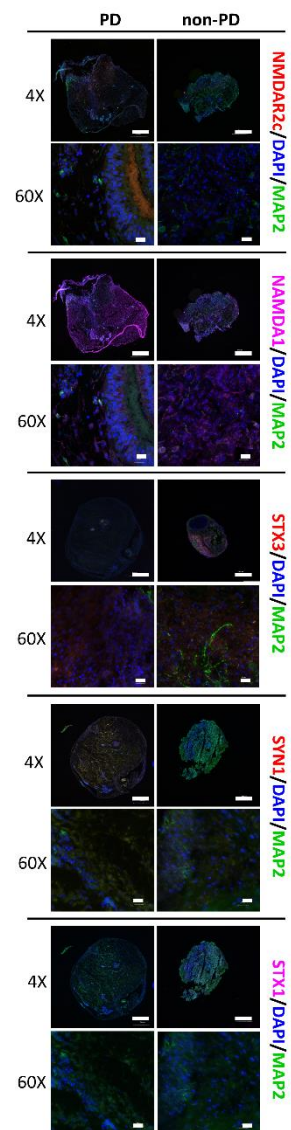
Eight genes associated with serotonin neurotransmission were examined. Here, PD organoids displayed increased expression of HTR2A, HTR3A, HTR3B and decreased expression of HTR7, MAOA and TPH1 (Figure 5A, Table S3). In non-PD organoids, HTR2A was down-regulated -2.42 logs, HTR3A was not differentially expressed and, HTR3B was up-regulated 6.52 logs (Figure 5A, Table S1). HTR1B and HTR1E were

down-regulated in non-PD organoids -1.46 and -2.98 logs, respectively while these targets were not differentially expressed in PD organoids (Figure 5A, Table S1, S3).

Thirty-six targets representing a spectrum of transporters involved in neurotransmission were examined.  $\Delta\Delta Ct$  values showed that non-PD organoids exhibited decreased expression of all targets except SLC6A16, SLC32A1, SLC6A7 (Figure 5A, Table S1).  $\Delta\Delta Ct$  values for PD organoids showed up-regulation of 5 SLC receptors which were down-regulated in non-PD organoids (Figure 5A, Table S1, S3). In non-PD organoids, RIMS 1, 3, and 4 were down-regulated while only RIMS4 was differentially expressed in PD organoids at an increase of 2.13 logs (Figure 5A, Table S1, S3). Synaptophilin (SNPH), Syntaxins (STX) 1A, 1B, 3 and synapsins (SYN) 1, 2, and 3 were significantly down-regulated in PD organoids while non-PD organoids were not differentially expressed for SYN1 and SYN3 (Figure 5A, Table S1, S3). Synaptophysin (SYP) and Synaptotagmin (SYT1) were also down-regulated in PD organoids more than 1 log when compared to infected non-PD organoids (Figure 5A, Table S1, S3).

Immunofluorescence for neurotransmission markers for glutamate receptors NMDA1 and NMDAR2c reflected gene expression data where PD organoids had less fluorescence of both markers compared to non-PD organoids (Figure 6). STX1 and STX3 fluorescence did not reflect gene expression data of decreased expression in both non-PD and PD organoids (Figure 6). PD organoids also had decreased fluorescence of SYN1 when compared to non-PD organoids which had increased expression (Figure 6).

**Figure 6.** Immunofluorescence of neurotransmission markers of PD and non-PD organoids infected with CHIKV. Immunofluorescence of neurotransmission targets in PD and non-PD organoids. Images were obtained to validate gene expression data. DAPI was used throughout to visualize nuclei and MAP2 was used to visualize microtubules to provide a structural reference. Images of organoids were obtained using an Olympus Fluoview3000 confocal microscope. Scale bar represents 500 nm for images obtained at 4X magnification and 20 nm for images obtained at 60X magnification.



### 2.3 Alterations in Immune Regulation

Both PD and non-PD organoids were evaluated for immune response to CHIKV infection. Markers included surface receptors, stress response, oxidoreductases, cytokines including multiple chemokine receptors, and markers for cell lysis. Overall, PD organoids exhibited increased expression of all markers evaluated on the array when compared with their non-infected control (Figure 4B).  $\Delta\Delta Ct$  analysis of both infected organoids types with the non-PD non-infected control showed a variable response for both organoid types. 24 of 27 markers for surface receptors were up-regulated in PD organoids including CD28 (10.11 logs), IL2RA (9.68 logs), PTPRC (8.71

logs) (Figure 5B, Table S3). PD organoids showed decreased expression for CD4 (-2.26 logs), CD40 (-4.36 logs), CD28 (-2.88 logs), IL2RA (-3.3 logs) and PTPRC (-1.29) (Figure 5B, Table S1). Of note, CD34 was down-regulated in non-PD organoids -8.82 logs but PD organoids were up-regulated 2.88 logs (Figure 5B, Table S1, S3). LY96 was down-regulated -7.55 logs in non-PD organoids but up-regulated 1.92 logs in PD organoids (Figure 5B, Table S1, S3).

Markers for stress response exhibited a similar pattern of expression for both organoids types though non-PD organoids were down-regulated -3.2 logs for AGTR2 while PD organoids were up-regulated 4.99 logs (Figure 5B, Table S1, S3). Further, C3 was up-regulated 1.51 logs in PD organoids but down-regulated in non-PD organoids -6.54 logs (Figure 5B, Table S1, S3). Non-PD organoids also exhibited significant down-regulation of colony stimulating factors 1- 3 as well as selectin E and P at a magnitude of at least 3 logs of PD organoids (Figure 5B, Table S1, S3). Oxidoreductases had a similar pattern of expression for both organoids type except HMOX1 which was up-regulated 1.02 logs in PD organoids but down-regulated -5.81 logs in non-PD organoids (Figure 5B, Table S1, S3).

Eight chemokine receptors were evaluated and here too, both organoids types had a similar expression pattern of up-regulation (Figure 5B). Of note, CCR5 was up-regulated 6.16 logs in PD organoids but down-regulated -3.4 logs in non-PD organoids (Figure 5B, Table S1, S3). CCR7 was down-regulated -7.82 logs in non-PD organoids but not differentially expressed in PD organoids (Figure 5B, Table S1, S3). PD organoids did not significantly express CXCR3 though non-PD organoids were down-regulated -3.03 logs (Figure 5B, Table S1, S3). Conversely, PD organoids were up-regulated 2.65 logs for PF4 but non-PD organoids were down-regulated -5.00 logs (Figure 5B, Table S1, S3).

Twenty-three surface receptors comprising a variety of interleukins, tumor necrosis factors, and chemokine ligands were evaluated. CCL2, CCL3, IL-6, IL-10, and TBX21 were significantly up-regulated in expression in PD organoids but down-regulated in non-PD organoids (Figure 5B, Table S1, S3). IL-1A, IL-1B, and IKBKB were down-regulated for both organoid types (Figure 5B, Table S1, S3). Both GZMB and PRF1 up-regulated in PD organoids but down-regulated in non-PD organoids (Figure 5B, Table S1, S3).

Immunofluorescence for immunological markers showed that ICAM was not detected by fluorescence in PD organoids and showed less CCR7 fluorescence than non-PD organoids (Figure 7). SELE had increased fluorescence in PD and non-PD organoids which does not reflect gene expression data (Figure 5B, Table S1, S3).

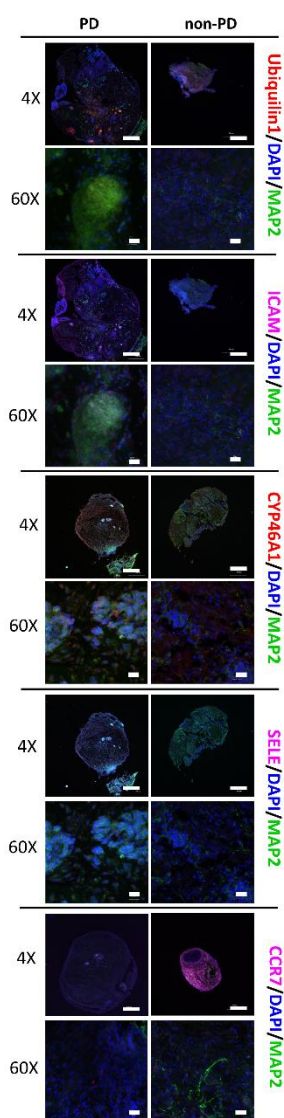


**Figure 7.** Immunofluorescence of immune markers in PD and non-PD organoids infected with CHIKV. Immunofluorescence of neurotransmission targets in PD and non-PD organoids. DAPI was used throughout to visualize nuclei and MAP2 was used to visualize microtubules to provide a structural reference. Images of organoids were obtained using an Olympus Fluoview3000 confocal microscope. Scale bar represents 500 nm for images obtained at 4X magnification and 20 nm for images obtained at 60X magnification.

#### 4. Discussion

Research of viral encephalitis and other viral infections of the CNS are crippled by necessary ethical restraints. This field relies on autopsy findings which are then typically applied to rodent models. Rodents do not present with symptoms of CNS pathologies unless they are genetically modified to be immune-deficient or have large quantities of virus administered via intracerebral injection or injection into other parts of the CNS. This has provided useful insights into the pathogenesis of these viruses, but unfortunately has not translated to treatment or prevention of human disease.

While animals are still valid and useful models, organoids can serve as a preliminary platform for screening which can better inform the design of animal studies and choice of genetic background. Ongoing advances with stem cell research have provided a platform for producing specific cell types or organoids from human stem cells. Within the last few years, significant advances in human health have been made using stem cells and organoids [35-39]. Human stem cells and organoids are emerging as a useful tool for virus research [40,41]. Not only do they replicate cellular composition and expression of humans, but they are also less expensive, safer, and easier to use than animals. Using organoids as a model can also produce better data due to the ability to have more replicates and numbers per treatment.

When infected with CHIKV, non-PD and PD organoids produced similar amounts of virus for the same period but after 2 weeks post-infection, PD organoids started to shrink. Immunofluorescence showed unique virus distribution patterns for non-PD and PD organoids. While non-PD organoids displayed uniform distribution of the CHIKV E1 protein, PD organoids exhibited local accumulation of CHIKV E1. Postmortem and necropsy data show focal distribution of West Nile virus in brain tissue [42,43]. Unfortunately, histological CNS data from CHIKV infected humans is not available since the role of CHIKV in neurological disease is an emerging topic [6,44,45]. Could the altered inflammatory response associated with PD contribute to the distribution of virus in the CNS and contribute to the establishment of chronic infection? In mice, CHIKV evades the CD8+ T-cell response to establish persistent infections [46]. Gene expression data show that IL-12 and IL-18 activate the CD8+ T-cell response [46]. It could be that the reduced expression of IL-12 and IL-18 in CHIKV-infected non-PD organoids is contributing to the infection

patterns we observed. CD4 and CD8 cells would need to be incorporated into this model to delineate how the innate immune response is impacting the activation of T cells.

The distribution and density of astrocytes in non-infected organoids is comparable to other studies that document organoid morphology [47,48]. GFAP was used to detect activated astrocytes. Histological studies have found that many mature astrocytes do not express significant GFAP unless activated [49]. Thus, the lack of staining observed in non-infected non-PD organoids is likely indicative that astrocytes are in an inactivated state. Staining of PD organoids showed extensive distribution of astrocytes with a section of astrogliosis. Non-PD infected organoids had astrocytes distributed solely on the outer margins which mimics other studies investigation astrocyte activation in organoids [47]. Neurofilament is a component of mature neuronal cytoskeleton often found in high concentrations in axons. In growing or developing neurons, neurofilament may not be readily apparent since younger axons are much smaller than mature neurons [50]. Imaging studies show neurofilament staining for all organoid types which suggests that organoids possess mature neuron populations. Statistical analysis was not performed for these images due to the non-uniform distribution of cell types (neuronal, glial, ependymal, etc.) between organoids.

SOX2 and Tuj1 were used to observe neuron proliferation in response to CHIKV. When compared to non-infected organoids, SOX2 fluorescence was similar in CHIKV-infected non-PD organoids but was reduced in CHIKV-infected PD organoids. SOX2 is a transcription factor that regulates pluripotency and neurogenesis and is integral to the growth and repair of neurons [51]. The reduced expression of SOX2 in infected PD organoids could mean that there is dysfunction in neuron growth however, detection of other assorted transcription factors would be necessary to understand the expression pattern.

$\Delta\Delta Ct$  was used to analyze changes in gene expression. When infected organoids were compared to their respective non-infected controls, PD organoids showed a pattern of up-regulation while non-PD organoids showed a pattern of down-regulation. While this is interesting in of itself, this analysis did not provide much insight as to whether PD organoids were mounting an antiviral response that reflected the response of non-PD organoids. Previous work has documented that endogenous expression of most genes is different for PD and non-PD cells and patients [32,34]. Thus, any changes, or lack thereof of PD organoids to viral insult may not reflect a typical antiviral response when compared to its non-infected counterpart. When  $\Delta\Delta Ct$  analysis was performed comparing infected PD organoids with a non-PD non-infected control, it was observed that both non-PD and PD organoids had similar expression patterns for most markers in response to CHIKV infection. This indicates that PD organoids modify their expression in response to virus infection for most markers and mount a response like non-PD organoids.

This study showed and overall pattern of excitation of GABA, glycine, glutamate, and serotonin receptors in PD organoids when infected with CHIKV. While non-PD organoids exhibited a decreased pattern of expression for the same markers. While it is well documented that CHIKV can cause long-term or permanent depressive sequelae, there are no studies describing changes in neurotransmission. Two studies have reported the potential antiviral activity of serotonergic drugs on CHIKV replication though viral inhibition assays though impacts on serotonin neurotransmission are not described [52,53]. GABRP, HTR3, SLC6A4, SLCA9 and SNPH were differentially expressed for both organoid

types. HTR3 receptors are associated with neuro-gastrointestinal and psychiatric conditions that are controlled with 5-HT3 receptor antagonists [54].

While the gene expression data shows that the response to CHIKV involves changes in neurotransmission and immune response. Clinical trials have shown that dysregulation of the inflammatory response can remodel neurotransmission leading the changes in mood and cognition [13,55,56]. The reduced expression of ACHE has been linked to depression and cognitive deficits in human studies [57-59]. Perhaps ACHE could be contributing to persistent depressive sequelae in CHIKV patients.

The data show that both PD organoids have increased expression of NFKB2, a transcription control protein that functions in the innate antiviral response [60]. In PD, NFKB2 is activated with IL-17 when cultured with T-lymphocytes [61]. Activation of NFKB2 results in the production of interferons which play a significant role in the innate antiviral response [60]. We also observed up-regulation of many proinflammatory cytokines in response to CHIKV infection in PD organoids when compared with non-PD organoids. CSF2, and CSF3 respond to infection by inducing inflammation and recruiting lymphocytes to the site of infection. Several viruses evade this immune response by blocking autophagy, thereby blocking monocyte differentiation and apoptosis [62,63].

Oxidoreductases determine MHC class I surface exposure and influence the activation of inflammation cascades. When found on the plasma membrane, oxidoreductases signal intracellular stress status to the immune system [100]. In particular, HMOX1 has antiviral activity with increased levels associated with clearance of infection [101; 102; 103]. Our data show that PD organoids had increased expression of HMOX1 while non-PD organoids had decreased expression. When present, HMOX1 interacts with IL-10 (also down-regulated in infected non-PD organoids) as an anti-inflammatory mechanism of the innate immune response [60]. Research has shown that Zika and Dengue viruses decrease host expression of HMOX1 as part of their antiviral response [101; 107]. The deficit of HMOX1 could be contributing to the persistence and pattern of CHIKV in the organoids.

Cytokines direct the innate immune response and play an important role in regulating the adaptive immune response. Specific cytokines can serve as biomarkers for viral infections [64]. Our data support that PD organoids have increased expression of IL-5, IL-6, and IL-10, indicating that there could be an activation of a Th2 response. However, IL-12 was also significantly up-regulated in PD organoids, which would favor a cell-mediated inflammatory response to stress or infection, as well as the activation of cytotoxic T lymphocytes. We observed significant down regulation of IL-18 and IL-1B in non-PD organoids. These interleukins catalyze the production of several proinflammatory cytokines and recruit immune cells to the site of microbial infections. IL-12 promotes protective immunity to a variety of viruses and IL-12 and IL-18 work together during the antiviral response [65]. With IL-12 up-regulated and expression of IL-18 and IL-1 down-regulated, both PD and non-PD organoids could be having dysfunctional antiviral response. Of note, Non-PD organoids had down regulation of IL-1 and IL-10 in response to CHIKV. This aligns with studies that have shown that reduced expression of IL-1 and IL-10 can exacerbate mental illness or psychotic episodes following infection with CHIKV [66-68].

Chemokines are a subset of cytokines that are activated in response to tissue damage as well as foreign proteins and antigens. Overproduction of chemokines is associated with a variety of autoimmune diseases. Most chemokines we examined were expressed at greater levels in PD than non-PD organoids at 14 days post infection. This state of inflammation could potentially cause complications for responding to viral infections. CCL19 is a chemokine that binds to the CCR7 receptor and acts to recruit dendritic cells. CCL19 was up-regulated in PD and non-PD organoids. CCR7 was down-regulated in non-PD organoids but up-regulated in PD organoids. The expression profiles of PD organoids reflect expression profiles documented from cerebrospinal fluid from patients infected with Varicella-Zoster virus [69]. Also, studies in CCR7 deficient mice reported increased death from West Nile virus infection via over-recruitment of leukocytes and inflammation [70]. The reduced activity of CCR7 we observed could render organoids vulnerable to neuropathogens due to enhanced expression towards an inflammatory response.

CCL3 interacts with CCR4 and CCR5 during the acute inflammatory response and functions to recruit monocytes which can have an impact on neuroimmunity [71]. The increased expression of CCL3 and CCL5 in both PD and non-PD organoids also occurs during infection with respiratory pathogens and is associated with severe manifestations of disease [72]. Animal studies support that expression of CCR5 is up-regulated in CNS infections with Japanese Encephalitis virus and positively correlated with increased pathogenesis [73]. Work has shown that increased levels of CCR5 contribute to demyelination and CNS disease [74]. The increased expression of CCR5 in PD organoids indicates that they are in an inflammatory state or could be experiencing neuronal damage.

The complement system is a part of the innate immune response that can lyse cells, activate inflammation, target virus to phagocytic cells, and clear non-cytopathic viruses from the circulatory system. Here, we evaluated the expression of C3 as it functions in both classical and alternative complement activation pathways and deficiency of C3 can make humans more susceptible to viral and bacterial infections [75,76]. In our study, PD organoids had increased in C3 expression compared with non-PD organoids suggesting a functional complement system. Non-PD organoids had down-regulation of C3 which has been reported in patients with Hepatitis C infection [75]. Functional expression of C3 is necessary to neutralize West Nile and other viruses which cause acute neurological infections and death [76,77]. This poses an important question to be addressed in future research: could a reduction in C3 leave patients with CHIKV disease primed for neurological sequelae?

The use of only 2 cell lines (1 non-PD, 1 PD) is a limitation of this study due to the extensive genetic variation of PD. There are nearly 400 hiPSC cell lines derived from PD patients available for research [23]. While typical neuronal studies utilize up to 5 cell lines per study (3 diseased, 2 control) the appropriate numbers of cell lines to use for brain organoid research is still under debate [23]. PD research utilizing organoids typically differentiate from 1 non-PD and 1 PD hiPSC line [48]. In depth analysis of preliminary concepts requires

substantial resources and time that is not justifiable for pilot studies, especially when generating organoids [23]. Thus, preliminary data is often limited to 2 cell lines (control and diseased) [108; 109; 110]. Regardless, the findings here need substantiation in organoids derived from additional cell lines.

## 5. Conclusions

The data show that neurophysiology is dramatically different between a non-PD and PD organoids and the response to viral infection is altered in PD organoids. This is of significant concern given the rising numbers of persons with neurodegenerative/neurological disease. Could viral infection with a neurotropic virus cause or exacerbate the development of neurological disease in persons predisposed for such conditions? The dysfunctional antiviral response of PD organoids highlights the need for more research in neurotropic infections in a neurologically compromised host.

**Supplementary Materials:** The following are available online at [www.mdpi.com/xxx/s1](http://www.mdpi.com/xxx/s1), **Table S1:** Gene expression data and analysis for non-PD organoids and non-PD organoids infected with CHIKV obtained 14 days post inoculation. UDT: undetermined

**Table S2.** Gene expression data and analysis for PD organoids and PD organoids infected with CHIKV obtained 14 days post inoculation. UDT: undetermined

**Table S3.** Gene expression data and analysis for non-PD organoids and PD organoids infected with CHIKV obtained 14 days post inoculation. UDT: undetermined

**Author Contributions:** Conceptualization, K.L.B.; methodology, K.L.B., E.M.S., D.D.D., B.Z.; validation, K.L.B., E.M.S.; formal analysis, K.L.B., E.M.S.; investigation, K.L.B., E.M.S.; resources, K.L.B.; data curation, K.L.B., E.M.S.; writing—original draft preparation, K.L.B., E.M.S.; writing—review and editing, K.L.B., E.M.S., T.J.J., S.X., D.D.D., B.Z.; visualization, K.L.B.; supervision, K.L.B.; project administration, K.L.B.; funding acquisition, K.L.B. All authors have read and agreed to the published version of the manuscript.”, please turn to the [CRediT taxonomy](#) for the term explanation.

**Funding:** This project was supported by start-up funds from Baylor University to Kelli L. Barr.

**Acknowledgments:** In this section you can acknowledge any support given which is not covered by the author contribution or funding sections. This may include administrative and technical support, or donations in kind (e.g., materials used for experiments).

**Conflicts of Interest:** The authors declare no conflict of interest.

## References

1. Jang, H.; Boltz, D.A.; Webster, R.G.; Smeyne, R.J. Viral parkinsonism. *Biochimica et biophysica acta* **2009**, *1792*, 714–721, doi:10.1016/j.bbadis.2008.08.001.
2. Weaver, S.C.; Winegar, R.; Manger, I.D.; Forrester, N.L. Alphaviruses: population genetics and determinants of emergence. *Antiviral research* **2012**, *94*, 242–257, doi:10.1016/j.antiviral.2012.04.002.
3. Rocklov, J.; Quam, M.B.; Sudre, B.; German, M.; Kraemer, M.U.G.; Brady, O.; Bogoch, I.; Liu-Helmersson, J.; Wilder-Smith, A.; Semenza, J.C., et al. Assessing Seasonal Risks for the Introduction and Mosquito-borne Spread of Zika Virus in Europe. *EBioMedicine* **2016**, *9*, 250–256, doi:10.1016/j.ebiom.2016.06.009 10.1016/j.ebiom.2016.06.009. Epub 2016 Jun 10.

4. Sooryanarain, H.; Elankumaran, S. Environmental role in influenza virus outbreaks. *Annu Rev Anim Biosci* **2015**, *3*, 347-373, doi:10.1146/annurev-animal-022114-111017.
5. Grassly, N.C.; Fraser, C. Seasonal infectious disease epidemiology. In *Proc Biol Sci*, 2006; Vol. 273, pp. 2541-2550.
6. Barr, K.L.; Khan, E.; Farooqi, J.Q.; Imtiaz, K.; Prakoso, D.; Malik, F.; Lednicky, J.A.; Long, M.T. Evidence of Chikungunya Virus Disease in Pakistan Since 2015 With Patients Demonstrating Involvement of the Central Nervous System. *Front Public Health* **2018**, *6*, 186, doi:10.3389/fpubh.2018.00186.
7. Barr, K.L.; Vaidhyanathan, V. Chikungunya in Infants and Children: Is Pathogenesis Increasing? *Viruses* **2019**, *11*, doi:10.3390/v11030294 10.3390/v11030294.
8. Sharma, S.; Tandel, K.; Dash, P.K.; Parida, M. Zika virus: A public health threat. *Journal of medical virology* **2017**, *89*, 1693-1699, doi:10.1002/jmv.24822.
9. Gregianini, T.S.; Ranieri, T.; Favreto, C.; Nunes, Z.M.A.; Tumioto Giannini, G.L.; Sanberg, N.D.; da Rosa, M.T.M.; da Veiga, A.B.G. Emerging arboviruses in Rio Grande do Sul, Brazil: Chikungunya and Zika outbreaks, 2014-2016. *Rev Med Virol* **2017**, *27*, doi:10.1002/rmv.1943.
10. Brault, A.C. Changing patterns of West Nile virus transmission: altered vector competence and host susceptibility. In *Vet Res*, 2009; Vol. 40.
11. Bakonyi, T.; Erdélyi, K.; Ursu, K.; Ferenczi, E.; Csörgo, T.; Lussy, H.; Chvala, S.; Bukovsky, C.; Meister, T.; Weissenböck, H., et al. Emergence of Usutu virus in Hungary. *J Clin Microbiol* **2007**, *45*, 3870-3874, doi:10.1128/JCM.01390-07.
12. Wang, H.; Liu, X.; Tan, C.; Zhou, W.; Jiang, J.; Peng, W.; Zhou, X.; Mo, L.; Chen, L. Bacterial, viral, and fungal infection-related risk of Parkinson's disease: Meta-analysis of cohort and case-control studies. *Brain Behav* **2020**, *10*, e01549, doi:10.1002/brb3.1549.
13. Abdoli, A.; Taghipour, A.; Pirestani, M.; Mofazzal Jahromi, M.A.; Roustazadeh, A.; Mir, H.; Ardakani, H.M.; Kenarkoobi, A.; Falahi, S.; Karimi, M. Infections, inflammation, and risk of neuropsychiatric disorders: the neglected role of "co-infection". *Heliyon* **2020**, *6*, e05645, doi:10.1016/j.heliyon.2020.e05645.
14. McLoone, P.; Dyussupov, O.; Nurtlessov, Z.; Kenessariyev, U.; Kenessary, D. The effect of exposure to crude oil on the immune system. Health implications for people living near oil exploration activities. *Int J Environ Health Res* **2019**, 10.1080/09603123.2019.1689232, 1-26, doi:10.1080/09603123.2019.1689232.
15. Zubcevic, J.; Jun, J.Y.; Kim, S.; Perez, P.D.; Afzal, A.; Shan, Z.; Li, W.; Santisteban, M.M.; Yuan, W.; Febo, M., et al. Altered inflammatory response is associated with an impaired autonomic input to the bone marrow in the spontaneously hypertensive rat. *Hypertension* **2014**, *63*, 542-550, doi:10.1161/HYPERTENSIONAHA.113.02722.
16. Cvejic, E.; Lemon, J.; Hickie, I.B.; Lloyd, A.R.; Vollmer-Conna, U. Neurocognitive disturbances associated with acute infectious mononucleosis, Ross River fever and Q fever: a preliminary investigation of inflammatory and genetic correlates. *Brain Behav Immun* **2014**, *36*, 207-214, doi:10.1016/j.bbi.2013.11.002.
17. Piraino, B.; Vollmer-Conna, U.; Lloyd, A.R. Genetic associations of fatigue and other symptom domains of the acute sickness response to infection. *Brain Behav Immun* **2012**, *26*, 552-558, doi:10.1016/j.bbi.2011.12.009.
18. Vollmer-Conna, U.; Piraino, B.F.; Cameron, B.; Davenport, T.; Hickie, I.; Wakefield, D.; Lloyd, A.R. Cytokine polymorphisms have a synergistic effect on severity of the acute sickness response to infection. *Clin Infect Dis* **2008**, *47*, 1418-1425, doi:10.1086/592967.
19. Bopeththa, B.; Ralapanawa, U. Post encephalitic parkinsonism following dengue viral infection. *BMC Res Notes* **2017**, *10*, 655, doi:10.1186/s13104-017-2954-5.

20. Robinson, R.L.; Shahida, S.; Madan, N.; Rao, S.; Khardori, N. Transient parkinsonism in West Nile virus encephalitis. *Am J Med* **2003**, *115*, 252-253, doi:10.1016/s0002-9343(03)00291-2.
21. Ogata, A.; Tashiro, K.; Pradhan, S. Parkinsonism due to predominant involvement of substantia nigra in Japanese encephalitis. *Neurology* **2000**, *55*, 602, doi:10.1212/wnl.55.4.602.
22. Cerna, F.; Mehrad, B.; Luby, J.P.; Burns, D.; Fleckenstein, J.L. St. Louis encephalitis and the substantia nigra: MR imaging evaluation. *AJNR Am J Neuroradiol* **1999**, *20*, 1281-1283.
23. Vilensky, J.A.; Duvosin, R.C.; Gilman, S. The diagnosis of postencephalitic parkinsonism at the neurological unit of Boston City Hospital, 1930-1981. *Neurological sciences : official journal of the Italian Neurological Society and of the Italian Society of Clinical Neurophysiology* **2011**, *32*, 343-346, doi:10.1007/s10072-011-0487-6.
24. Takahashi, M.; Yamada, T. Viral etiology for Parkinson's disease--a possible role of influenza A virus infection. *Japanese journal of infectious diseases* **1999**, *52*, 89-98.
25. Caggiu, E.; Arru, G.; Hosseini, S.; Niegowska, M.; Sechi, G.; Zarbo, I.R.; Sechi, L.A. Inflammation, Infectious Triggers, and Parkinson's Disease. *Frontiers in Neurology* **2019**, *10*, doi:10.3389/fneur.2019.00122.
26. Schultz, E.M.; Jones, T.; Xu, S.; Dean, D.; Zechmann, B.; Ronca, S.; Barr, K.L. Differences between Cerebral Organoids Derived from a non-PD and a Parkinson's Patient: A Potential Vulnerability for Neuroinvasive Viruses *Biology* **2021**, *10.20944/preprints202101.0480.v1*, doi:10.20944/preprints202101.0480.v1.
27. Ghatak, S.; Dolatabadi, N.; Trudler, D.; Zhang, X.; Wu, Y.; Mohata, M.; Ambasudhan, R.; Talantova, M.; Lipton, S.A. Mechanisms of hyperexcitability in Alzheimer's disease hiPSC-derived neurons and cerebral organoids vs isogenic controls. *eLife* **2019**, *8*, e50333, doi:10.7554/eLife.50333.
28. Ao, Z.; Cai, H.; Havert, D.J.; Wu, Z.; Gong, Z.; Beggs, J.M.; Mackie, K.; Guo, F. One-Stop Microfluidic Assembly of Human Brain Organoids To Model Prenatal Cannabis Exposure. *Analytical chemistry* **2020**, *92*, 4630-4638, doi:10.1021/acs.analchem.0c00205.
29. Marx, V. Reality check for organoids in neuroscience. *Nature Methods* **2020**, *17*, 961-964, doi:10.1038/s41592-020-0964-z.
30. Dutta, D.; Clevers, H. Organoid culture systems to study host-pathogen interactions. *Current opinion in immunology* **2017**, *48*, 15-22, doi:10.1016/j.coi.2017.07.012.
31. Papariello, A.; Newell-Litwa, K. Human-Derived Brain Models: Windows Into Neuropsychiatric Disorders and Drug Therapies. *Assay and drug development technologies* **2019**, *10.1089/adt.2019.922* 10.1089/adt.2019.922., doi:10.1089/adt.2019.922 10.1089/adt.2019.922.
32. Tran, J.; Anastacio, H.; Bardy, C. Genetic predispositions of Parkinson's disease revealed in patient-derived brain cells. *NPJ Parkinson's disease* **2020**, *6*, 8, doi:10.1038/s41531-020-0110-8.
33. Kouroupi, G.; Taoufik, E.; Vlachos, I.S.; Tsiaras, K.; Antoniou, N.; Papastefanaki, F.; Chroni-Tzartou, D.; Wrasidlo, W.; Bohl, D.; Stellas, D., et al. Defective synaptic connectivity and axonal neuropathology in a human iPSC-based model of familial Parkinson's disease. *Proc Natl Acad Sci U S A* **2017**, *114*, E3679-e3688, doi:10.1073/pnas.1617259114.
34. Lin, L.; Göke, J.; Cukuroglu, E.; Dranias, M.R.; VanDongen, A.M.; Stanton, L.W. Molecular Features Underlying Neurodegeneration Identified through In Vitro Modeling of Genetically Diverse Parkinson's Disease Patients. *Cell Rep* **2016**, *15*, 2411-2426, doi:10.1016/j.celrep.2016.05.022.
35. Goureau, O.; Orieux, G. [Photoreceptor cell transplantation for future treatment of retinitis pigmentosa]. *Med Sci (Paris)* **2020**, *36*, 600-606, doi:10.1051/medsci/2020097.

36. Youhanna, S.; Lauschke, V.M. The Past, Present and Future of Intestinal In Vitro Cell Systems for Drug Absorption Studies. *J Pharm Sci* **2020**, 10.1016/j.xphs.2020.07.001, doi:10.1016/j.xphs.2020.07.001.
37. Yuki, K.; Cheng, N.; Nakano, M.; Kuo, C.J. Organoid Models of Tumor Immunology. *Trends Immunol* **2020**, *41*, 652-664, doi:10.1016/j.it.2020.06.010.
38. Zanoni, M.; Cortesi, M.; Zamagni, A.; Arienti, C.; Pignatta, S.; Tesei, A. Modeling neoplastic disease with spheroids and organoids. *J Hematol Oncol* **2020**, *13*, 97, doi:10.1186/s13045-020-00931-0.
39. Oltra, J.A.E. Improving Therapeutic Interventions of Schizophrenia with Advances in Stem Cell Technology. *Clin Psychopharmacol Neurosci* **2020**, *18*, 352-361, doi:10.9758/cpn.2020.18.3.352.
40. Makovoz, B.; Moeller, R.; Zebitz Eriksen, A.; tenOever, B.R.; Blenkinsop, T.A. SARS-CoV-2 Infection of Ocular Cells from Human Adult Donor Eyes and hESC-Derived Eye Organoids. *Ssrn* **2020**, 10.2139/ssrn.3650574, 3650574, doi:10.2139/ssrn.3650574.
41. Wong, Y.C.; Lau, S.Y.; Wang To, K.K.; Mok, B.W.Y.; Li, X.; Wang, P.; Deng, S.; Woo, K.F.; Du, Z.; Li, C., et al. Natural transmission of bat-like SARS-CoV-2<sup>PRRA</sup> variants in COVID-19 patients. *Clin Infect Dis* **2020**, 10.1093/cid/ciaa953, doi:10.1093/cid/ciaa953.
42. Smedley, R.C.; Patterson, J.S.; Miller, R.; Massey, J.P.; Wise, A.G.; Maes, R.K.; Wu, P.; Kaneene, J.B.; Kiupel, M. Sensitivity and specificity of monoclonal and polyclonal immunohistochemical staining for West Nile virus in various organs from American crows (*Corvus brachyrhynchos*) 120. *BMC Infect Dis* **2007**, *7*, 49.
43. Armah, H.B.; Wang, G.; Omalu, B.I.; Tesh, R.B.; Gyure, K.A.; Chute, D.J.; Smith, R.D.; Dulai, P.; Vinters, H.V.; Kleinschmidt-DeMasters, B.K., et al. Systemic Distribution of West Nile Virus Infection: Postmortem Immunohistochemical Study of Six Cases. *Brain Pathology* **2007**, *17*, 354-362, doi:10.1111/j.1750-3639.2007.00080.x.
44. Sá, P.K.O.; Nunes, M.M.; Leite, I.R.; Campelo, M.D.G.L.; Leão, C.F.R.; Souza, J.R.; Castellano, L.R.; Fernandes, A.I.V. Chikungunya virus infection with severe neurologic manifestations: report of four fatal cases. *Rev Soc Bras Med Trop* **2017**, *50*, 265-268, doi:10.1590/0037-8682-0375-2016.
45. Cerny, T.; Schwarz, M.; Schwarz, U.; Lemant, J.; Gérardin, P.; Keller, E. The Range of Neurological Complications in Chikungunya Fever. *Neurocrit Care* **2017**, 10.1007/s12028-017-0413-8, doi:10.1007/s12028-017-0413-8.
46. Davenport, B.J.; Bullock, C.; McCarthy, M.K.; Hawman, D.W.; Murphy, K.M.; Kedl, R.M.; Diamond, M.S.; Morrison, T.E. Chikungunya Virus Evades Antiviral CD8(+) T Cell Responses To Establish Persistent Infection in Joint-Associated Tissues. *Journal of virology* **2020**, *94*, e02036-02019, doi:10.1128/JVI.02036-19.
47. Huang, J.; Liu, F.; Tang, H.; Wu, H.; Li, L.; Wu, R.; Zhao, J.; Wu, Y.; Liu, Z.; Chen, J. Tranylcypromine Causes Neurotoxicity and Represses BHC110/LSD1 in Human-Induced Pluripotent Stem Cell-Derived Cerebral Organoids Model. *Front Neurol* **2017**, *8*, 626, doi:10.3389/fneur.2017.00626.
48. Dezone, R.S.; Sartore, R.C.; Nascimento, J.M.; Saia-Cereda, V.M.; Romão, L.F.; Alves-Leon, S.V.; de Souza, J.M.; Martins-de-Souza, D.; Rehen, S.K.; Gomes, F.C. Derivation of Functional Human Astrocytes from Cerebral Organoids. *Sci Rep* **2017**, *7*, 45091, doi:10.1038/srep45091.
49. Sofroniew, M.V.; Vinters, H.V. Astrocytes: biology and pathology. *Acta neuropathologica* **2010**, *119*, 7-35, doi:10.1007/s00401-009-0619-8.
50. B., A.; A., J.; J., L. *Molecular Biology of the Cell*, 4 ed.; Garland Science: New York, 2002.
51. Holmes, Z.E.; Hamilton, D.J.; Hwang, T.; Parsonnet, N.V.; Rinn, J.L.; Wuttke, D.S.; Batey, R.T. The Sox2 transcription factor binds RNA. *Nature communications* **2020**, *11*, 1805, doi:10.1038/s41467-020-15571-8.

52. Bouma, E.M.; van de Pol, D.P.I.; Sanders, I.D.; Rodenhuis-Zybert, I.A.; Smit, J.M. Serotonergic Drugs Inhibit Chikungunya Virus Infection at Different Stages of the Cell Entry Pathway. *J Virol* **2020**, *94*, doi:10.1128/jvi.00274-20.
53. Mainou, B.A.; Ashbrook, A.W.; Smith, E.C.; Dorset, D.C.; Denison, M.R.; Dermody, T.S. Serotonin Receptor Agonist 5-Nonyloxytryptamine Alters the Kinetics of Reovirus Cell Entry. *J Virol* **2015**, *89*, 8701-8712, doi:10.1128/jvi.00739-15.
54. Celli, J.; Rappold, G.; Niesler, B. The Human Serotonin Type 3 Receptor Gene (HTR3A-E) Allelic Variant Database. *Human mutation* **2017**, *38*, 137-147, doi:10.1002/humu.23136.
55. Culibrk, R.A.; Hahn, M.S. The Role of Chronic Inflammatory Bone and Joint Disorders in the Pathogenesis and Progression of Alzheimer's Disease. *Front Aging Neurosci* **2020**, *12*, 583884, doi:10.3389/fnagi.2020.583884.
56. Mészáros, Á.; Molnár, K.; Nógrádi, B.; Hernádi, Z.; Nyúl-Tóth, Á.; Wilhelm, I.; Krizbai, I.A. Neurovascular Inflammation in Health and Disease. *Cells* **2020**, *9*, doi:10.3390/cells9071614.
57. Suarez-Lopez, J.R.; Hood, N.; Suárez-Torres, J.; Gahagan, S.; Gunnar, M.R.; López-Paredes, D. Associations of acetylcholinesterase activity with depression and anxiety symptoms among adolescents growing up near pesticide spray sites. *Int J Hyg Environ Health* **2019**, *222*, 981-990, doi:10.1016/j.ijheh.2019.06.001.
58. Yanez, M.; Vina, D. Dual inhibitors of monoamine oxidase and cholinesterase for the treatment of Alzheimer disease. *Current topics in medicinal chemistry* **2013**, *13*, 1692-1706.
59. Suarez-Lopez, J.R.; Himes, J.H.; Jacobs, D.R., Jr.; Alexander, B.H.; Gunnar, M.R. Acetylcholinesterase activity and neurodevelopment in boys and girls. *Pediatrics* **2013**, *132*, e1649-1658, doi:10.1542/peds.2013-0108.
60. Häcker, H.; Karin, M. Regulation and function of IKK and IKK-related kinases. *Sci STKE* **2006**, *2006*, re13, doi:10.1126/stke.3572006re13.
61. Sommer, A.; Marxreiter, F.; Krach, F.; Fadler, T.; Grosch, J.; Maroni, M.; Graef, D.; Eberhardt, E.; Riemenschneider, M.J.; Yeo, G.W., et al. Th17 Lymphocytes Induce Neuronal Cell Death in a Human iPSC-Based Model of Parkinson's Disease. *Cell stem cell* **2018**, *23*, 123-131.e126, doi:10.1016/j.stem.2018.06.015.
62. Gilardini Montani, M.S.; Santarelli, R.; Granato, M.; Gonnella, R.; Torrisi, M.R.; Faggioni, A.; Cirone, M. EBV reduces autophagy, intracellular ROS and mitochondria to impair monocyte survival and differentiation. *Autophagy* **2019**, *15*, 652-667, doi:10.1080/15548627.2018.1536530.
63. Santarelli, R.; Granato, M.; Faggioni, A.; Cirone, M. Interference with the Autophagic Process as a Viral Strategy to Escape from the Immune Control: Lesson from Gamma Herpesviruses. *J Immunol Res* **2015**, *2015*, 546063-546063, doi:10.1155/2015/546063.
64. Papa, A.; Tsergouli, K.; Çağlayık, D.Y.; Bino, S.; Como, N.; Uyar, Y.; Korukluoglu, G. Cytokines as biomarkers of Crimean-Congo hemorrhagic fever. *J Med Virol* **2016**, *88*, 21-27, doi:10.1002/jmv.24312.
65. Gherardi, M.M.; Ramírez, J.C.; Esteban, M. IL-12 and IL-18 act in synergy to clear vaccinia virus infection: involvement of innate and adaptive components of the immune system. *J Gen Virol* **2003**, *84*, 1961-1972, doi:10.1099/vir.0.19120-0.
66. Figueiredo, T.; Dias da Costa, M.; Segenreich, D. Manic Episode After a Chikungunya Virus Infection in a Bipolar Patient Previously Stabilized With Valproic Acid. *J Clin Psychopharmacol* **2018**, *38*, 395-397, doi:10.1097/jcp.0000000000000887.

67. Michlmayr, D.; Pak, T.R.; Rahman, A.H.; Amir, E.D.; Kim, E.Y.; Kim-Schulze, S.; Suprun, M.; Stewart, M.G.; Thomas, G.P.; Balmaseda, A., et al. Comprehensive innate immune profiling of chikungunya virus infection in pediatric cases. *Molecular systems biology* **2018**, *14*, e7862, doi:10.15252/msb.20177862.
68. Rodriguez-Morales, A.J.; Hernandez-Moncada, A.M.; Hoyos-Guapacha, K.L.; Vargas-Zapata, S.L.; Sanchez-Zapata, J.F.; Mejia-Bernal, Y.V.; Ocampo-Serna, S.; Meneses-Quintero, O.M.; Gutierrez-Segura, J.C. Potential relationships between chikungunya and depression: Solving the puzzle with key cytokines. *Cytokine* **2018**, *102*, 161-162, doi:10.1016/j.cyto.2017.08.011.
69. Lind, L.; Eriksson, K.; Grahn, A. Chemokines and matrix metalloproteinases in cerebrospinal fluid of patients with central nervous system complications caused by varicella-zoster virus. *J Neuroinflammation* **2019**, *16*, 42, doi:10.1186/s12974-019-1428-1.
70. Bardina, S.V.; Brown, J.A.; Michlmayr, D.; Hoffman, K.W.; Sum, J.; Pletnev, A.G.; Lira, S.A.; Lim, J.K. Chemokine Receptor Ccr7 Restricts Fatal West Nile Virus Encephalitis. *J Virol* **2017**, *91*, doi:10.1128/jvi.02409-16.
71. Cheng, W.; Zhao, Q.; Xi, Y.; Li, C.; Xu, Y.; Wang, L.; Niu, X.; Wang, Z.; Chen, G. IFN- $\beta$  inhibits T cells accumulation in the central nervous system by reducing the expression and activity of chemokines in experimental autoimmune encephalomyelitis. *Mol Immunol* **2015**, *64*, 152-162, doi:10.1016/j.molimm.2014.11.012.
72. Russell, C.D.; Unger, S.A.; Walton, M.; Schwarze, J. The Human Immune Response to Respiratory Syncytial Virus Infection. *Clin Microbiol Rev* **2017**, *30*, 481-502, doi:10.1128/cmr.00090-16.
73. Zhang, F.; Qi, L.; Li, T.; Li, X.; Yang, D.; Cao, S.; Ye, J.; Wei, B. PD1(+)/CCR2(+)/CD8(+) T Cells Infiltrate the Central Nervous System during Acute Japanese Encephalitis Virus Infection. *Virol Sin* **2019**, *34*, 538-548, doi:10.1007/s12250-019-00134-z.
74. Li, F.; Cheng, B.; Cheng, J.; Wang, D.; Li, H.; He, X. CCR5 blockade promotes M2 macrophage activation and improves locomotor recovery after spinal cord injury in mice. *Inflammation* **2015**, *38*, 126-133, doi:10.1007/s10753-014-0014-z.
75. Mazumdar, B.; Kim, H.; Meyer, K.; Bose, S.K.; Di Bisceglie, A.M.; Ray, R.B.; Ray, R. Hepatitis C virus proteins inhibit C3 complement production. *J Virol* **2012**, *86*, 2221-2228, doi:10.1128/jvi.06577-11.
76. Avirutnan, P.; Hahart, R.E.; Marovich, M.A.; Garred, P.; Atkinson, J.P.; Diamond, M.S. Complement-mediated neutralization of dengue virus requires mannose-binding lectin. *mBio* **2011**, *2*, doi:10.1128/mBio.00276-11.
77. Fuchs, A.; Lin, T.Y.; Beasley, D.W.; Stover, C.M.; Schwaeble, W.J.; Pierson, T.C.; Diamond, M.S. Direct Complement Restriction of Flavivirus Infection Requires Glycan Recognition by Mannose-Binding Lectin. *Cell Host & Microbe* **2010**, *8*, 186-195, doi:10.1016/j.chom.2010.07.007.